



# Mapping of Possible Binding Sequences of Two Beta-Sheet Breaker Peptides on Beta Amyloid Peptide of Alzheimer's Disease

Csaba Hetényi,<sup>a,\*</sup> Tamás Körtvélyesi<sup>b,c</sup> and Botond Penke<sup>a</sup>

<sup>a</sup>Department of Medical Chemistry, University of Szeged, Dóm tér 8,  
H-6720 Szeged, Hungary

<sup>b</sup>Department of Physical Chemistry, University of Szeged, PO Box 105, H-6720 Szeged, Hungary

<sup>c</sup>Department of Biomedical Engineering, Boston University, 44 Cummington St, Boston, MA 02215, USA

Received 9 July 2001; accepted 30 November 2001

**Abstract**—Aggregation of amyloid peptide (A $\beta$ ) has been identified as a major feature of the pathogenesis of Alzheimer's disease. Increased risk for disease is associated with increased formation of polymerized A $\beta$ . Inhibition of formation of toxic (aggregated) form of A $\beta$  is one of the therapeutic possibilities. Beta sheet breaker peptides (BSBs) fulfill the requirements of an effective inhibitor. After having attached to the A $\beta$  molecules, BSBs can prevent aggregation of A $\beta$  to polymeric forms (aggregates). In the present study, we performed molecular modelling of complex formation between A $\beta$  and two BSB peptides. Our aim was to find proper binding sequences for the BSB peptides on A $\beta$  and characterize them. A dimeric model of A $\beta$  was also used to study the interaction of BSBs with the aggregated forms of A $\beta$  and find the sequences responsible for the polymerization process. A fast and efficient computational method: molecular docking was used for the afore-mentioned purposes. © 2002 Elsevier Science Ltd. All rights reserved.

## Introduction

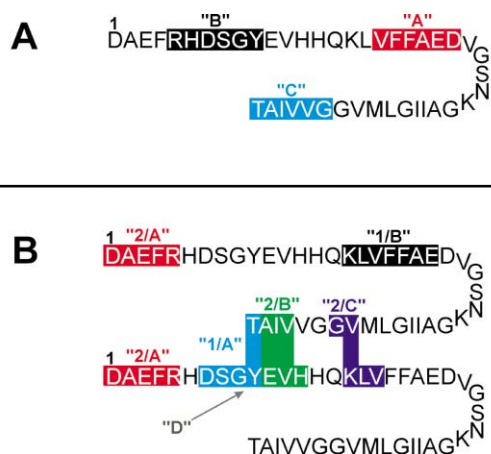
Senile dementia of the Alzheimer type can be characterized with neuritic plaques in the brain containing extracellular amyloid  $\beta$ -protein (A $\beta$ ) deposits. A $\beta$  occurs principally in fibrils and the main component of this filamentous form is a polypeptide chain of 42 amino acids (A $\beta_{1-42}$ ) which is particularly prone to aggregation.<sup>1</sup> The most abundantly produced 40 amino acid amyloid polypeptide (A $\beta_{1-40}$ ) shows limited aggregation, while the 43 amino acid form (A $\beta_{1-43}$ ) is the most rapidly aggregating natural sequence. A $\beta_{1-40}$  and A $\beta_{1-42/3}$  are co-localized in aggregated form in the neuritic plaques. Aggregated A $\beta$  proteins are neurotoxic by triggering Ca<sup>2+</sup>-influx into the neurons, free radical formation and apoptosis.<sup>2</sup> Though, the steric structure of amyloid fibrils is not fully understood, NMR data show parallel  $\beta$ -sheet structure.<sup>3</sup> This is supported by computational modeling, which allows the presence of both parallel and antiparallel  $\beta$ -structure.<sup>4</sup> Detailed

summary of results of the investigations on the structure of amyloid fibrils can be found in ref 5.

Some peptides and non-peptidic compounds prevent formation of  $\beta$ -structure and amyloid aggregation (polymerization). These are the so-called  $\beta$ -sheet breakers (BSBs) and are considered to be potential drugs of Alzheimer's disease (for more information, see review of Findeis<sup>6</sup>). Well-known BSB-peptides were prepared by Tjernberg et al.<sup>7</sup> and Soto et al.<sup>8</sup>

Design of BSB peptides requires the precise knowledge of binding sequences on A $\beta$  proteins. Unfortunately, no high-resolution X-ray diffraction data of amyloid structures exist for molecular design. However, on the basis of experimental data, George and Howlett<sup>9</sup> published a very useful, computationally derived structural model for A $\beta$  and the fibrillar structure ('solid-state model' in ref 9) of A $\beta$  aggregates. In the recent study, we used their amyloid model as a target for docking simulations. Employing the automated computational algorithm (docking), our aim was to map the possible sequences of A $\beta$  which bind to BSB peptides with high affinity, and therefore, could be critical for the design of new BSBs.

\*Corresponding author. Tel.: +36-62545136; fax: +36-62545971;  
e-mail: csabahete@yahoo.com



**Scheme 1.** Schematic representation of the monomer (A) and dimer (B) form of A $\beta_{1-43}$  (target molecule). The different active sequences are marked with different colours and denoted according to text.

## Results and Discussion

### Docking of Tjernberg's peptide (KLVFF) and Soto's peptide (LPFFD) to the monomeric A $\beta_{1-43}$ (Target I)

Both KLVFF and LPFFD peptides contain two phenylalanine and charged amino acids (lysine and aspartic acid) which might be essential in the formation of aromatic interactions and salt bridges between the small BSB (ligand) peptides and the A $\beta_{1-43}$  (target) peptide. These features of KLVFF and LPFFD peptides were originally<sup>10</sup> predicted to be essential in their BSB effect. However, no attempt but one<sup>11</sup> was made till this time to show the possible details of the action of these peptides at atomic level and to check the original hypotheses. [It should be stressed, that in our former study,<sup>11</sup> we used a basically different target molecule and docking algorithm (Monte-Carlo method/simulated annealing instead of LGA) for modelling this problem.]

Sequences of A $\beta_{1-43}$  found to be active in the interactions with the BSBs are listed in Table 1. As three different grid maps were used for docking simulations, Table 1 contains data derived from 600 separate docking runs. [It was also possible to study the effect of the choice of grid size and spacing on the docking results, i.e., whether the basic conclusions drawn from one set of 100 runs differ from the other ones or not. Basically only a few differences can be found in the active sequences of A $\beta_{1-43}$  for KLVFF or LPFFD at grid maps 'A', 'B' or 'C' (see Methods for definition of letter codes.)] Energetically, a sequence may be more or less favourable than another one for different grid maps (see  $E_{\text{docked}}$  values of Table 1). However, these energy values had a limited use in this study: for selection of the energetically favourable complexes among the 100 runs. (See also section 'Verification of the significance of resulted binding sequences' for more details of energetics.)

The following sequences were found to be generally important in the interactions: (A) V(18)...D(23); (B) R(5)...Y(10); (C) G(38)...T(43) (Scheme 1A).

(A) **The V(18)...D(23) sequence.** According to the docking results, the V(18)...D(23) sequence seems to be one of the most common active sites of A $\beta_{1-43}$  for both KLVFF and LPFFD peptides. This sequence proved to have the highest populations ( $N$  up to 19) and also good energy values among the 100 runs (first, second or third lowest energies of the 5–6 groups tabulated in each cell of Table 1). Interestingly, this region of A $\beta_{1-43}$  has been used as a template for the design of both BSB peptides in the original papers.<sup>7,8</sup> Experimental evidence was published for the interaction of A $\beta_{16-22}$  peptide with itself: the *N*-acetyl-KLVFFA $\text{E-NH}_2$  fragments aggregate to form fibril similarly to A $\beta_{1-42/43}$ . Moreover, multiple quantum (MQ) NMR results<sup>12</sup> supported antiparallel orientation of the A $\beta_{16-22}$  peptides in the fibrils. Our docking results are in good agreement with these experimental findings: (1) the activity of the sequence V(18)...D(23) and (2) in some cases even the antiparallel alignment of KLVFF and the corresponding V(18)...D(23) sequence were also found (Fig. 1).

(B) **R(5)...Y(10).** This sequence was also found by the docking simulations of both LPFFD and KLVFF peptides several times, with very good energy scores in the case of LPFFD (grid maps 'A' and 'B'). However, the populations ( $N$ ) of these groups were lower than that of the V(18)...D(23) sequence was. The complex of R(5)...Y(10) [+ T(43)] sequence of A $\beta_{1-43}$  peptide and LPFFD is presented in Figure 2. Several H-bonds: **a**, **b**, **c**, **d**, **f** and a salt bridge between the end groups of the peptides (**e**) have stabilizing effect on this associate. KLVFF interacts with this sequence in a similar manner (via H-bonds and electrostatic interactions).

(C) **The G(38)...T(43) fragment.** There are several papers (e.g., refs<sup>13–15</sup>) indicating the importance of the end sequences of A $\beta$ . According to the present docking results, both Tjernberg's and Soto's BSB peptide dock to (part of) this sequence with relatively good energy scores and/or frequencies ( $N$  up to 13). Generally, amino acids with serial number Y(10)...H(13) are also involved in the interactions of this type. (These are the closest amino acids in this 'hairpin' model of A $\beta_{1-43}$ ; see Scheme 1A.) T is crucial in the forming of salt bridge between T(43) of A $\beta_{1-43}$  and the BSB peptide and in H-bonds (the latter formed by backbone CONH groups too). Interactions between non-polar groups strengthen the overall stability of the associate.

### Verification of the significance of resulted binding sequences

**Docking of 'blank' peptides.** To achieve some information on the significance of  $E_{\text{docked}}$  values of Tables 1 and 2, molecular docking experiments were performed on the monomer target for the AAAAA and AAVFA penta-peptides. AAVFA was constructed according to the experimental findings of ref 7, while AAAAA was used as an indifferent peptide and to estimate the contribution of the ionic end-groups and the backbone amide groups to the final  $E_{\text{docked}}$  values. The energy differences of the closest conformations of the blank peptides and the BSB peptides were calculated for the above-mentioned three main interacting sequences of the monomer

**Table 1.** Possible binding sequences of Tjernberg's peptide (**KLVFF**) and Soto's peptide (**LPFFD**) found by docking simulations on the monomer A $\beta_{1-43}$  peptide and the corresponding docked energies ( $E_{\text{docked}}$ ) of the complexes<sup>a</sup>

Peptide	Grid map 'A'			Grid map 'B'			Grid map 'C'		
	Binding sequence	<i>N</i>	$E_{\text{docked}}$ (kcal/mol)	Binding sequence	<i>N</i>	$E_{\text{docked}}$ (kcal/mol)	Binding sequence	<i>N</i>	$E_{\text{docked}}$ (kcal/mol)
Tjernberg's <b>KLVFF</b>	G(38)...A(42)+Y(10)E(11)	13	−9.7	V(40)...T(43)+G(9)...H(13)	4	−10.1	E(3)...Y(10)	4	−9.6
	V(40)...T(43)+S(8)	6	−8.3	H(13)...V(18)	3	−9.5	R(5)...E(11)	3	−9.5
	V(18)...E(22)	8	−8.1	E(3)...G(9)	4	−8.7	V(18)...E(22)	10	−9.4
	Q(15)...F(20)	11	−7.8	R(5)...Y(10)+T(43)	3	−8.4	V(18)...D(23)	3(11)*	−9.3
	A(42)T(43)+Y(10)...H(13)	9	−7.8	S(8)...E(11)	3	−8.3	R(5)...Y(10)+T(43)	3	−9.2
	D(7)...E(11)	4	−7.7				G(38)...A(42)+E(11)...H(13)	3	−8.7
Soto's <b>LPFFD</b>	R(5)...Y(10)+T(43)	2(7)*	−10.5	R(5)...Y(10)+T(43)	4	−11.1	V(18)...D(23)	10	−11.3
	L(17)...D(23)	19	−10.2	V(18)...D(23)	6	−11.1	E(11)...Q(15)+G(38)...I(41)	9	−11.0
	E(3)...S(8)	6	−9.7	V(18)...E(22)	7	−11.1	V(18)...E(22)	8	−10.8
	G(38)...A(42)+V(12)H(13)	8	−9.7	K(28)...L(34)	3	−10.4	V(40)...T(43)+Y(10)	7	−10.5
	R(5)...Y(10)+T(43)	4	−9.3				Y(10)...H(14)	3	−10.1

<sup>a</sup>Letters **A**, **B** and **C** denote grid maps with different sizes (see Methods for letter codes). The number of conformations docked to the same sequences of A $\beta_{1-43}$  is denoted with **N** (see text for further description). Numbers (*N*) of some conformations of the same binding sequences but of lower energies are marked with asterisk.

**Table 2.** Typical binding sequences of Tjernberg's peptide (**KLVFF**) and Soto's peptide (**LPFFD**) found by docking simulations on the dimeric form of A $\beta_{1-43}$  peptide and the corresponding docked energies ( $E_{\text{docked}}$ ) of the complexes<sup>a</sup>

Peptide	Grid map 'A'			Grid map 'B'			Grid map 'C'		
	Binding sequence	Location	$E_{\text{docked}}$ (kcal/mol)	Binding sequence	Location	$E_{\text{docked}}$ (kcal/mol)	Binding sequence	Location	$E_{\text{docked}}$ (kcal/mol)
Tjernberg's <b>KLVFF</b>	D(7)...Y(10)+T(43)	I	−11.2	D(7)...Y(10)+T(43)	I	−12.9	S(8)...E(11)+V(40)...T(43)	I, P	−11.2
	D(1)...R(5)	P	−10.8	E(11)...Q(15)+V(39)...T(43)	P	−10.8	R(5)...E(11)+I(41)...T(43)	I, P	−11.0
	Y(10)...H(13)+V(40)...T(43)	P	−9.9	A(21)...D(23)+K(28)...A(30)	P	−10.5	F(4)...Y(10)+T(43)	I	−10.9
	K(16)...V(18)+V(36)...G(37)	P	−9.1	G(9)...H(13)+T(43)	P	−10.0	K(16)...D(22)	I	−10.0
	A(2)...G(9)	I	−8.9	F(4)...D(7)	P	−9.9	F(20)...A(30)	P	−9.9
	G(37)...A(42)+G(11)...H(13)	P	−8.8				H(13)...Q(15)+G(36)...V(38)	P	−9.8
Soto's <b>LPFFD</b>	R(5)...Y(10)	I	−12.9	D(1)...R(5)	P	−12.8	R(5)...E(11)	I	−14.2
	H(6)...Y(10)+T(43)	I	−10.8	F(4)...Y(10)+T(43)	I	−12.1	D(7)...Y(10)+T(43)	I	−12.5
	Y(10)...H(13)+V(40)...T(43)	I	−10.6	S(8)...H(14)+V(40)...T(43)	I, P	−11.4	Y(10)...H(13)+V(40)...T(43)	P	−12.5
	V(24)...A(30)	P	−10.0	H(6)...Y(10)	I	−11.4	H(6)...Y(10)	I	−11.9
	D(1)...R(5)	P	−10.0	Y(10)...H(13)+I(41)...T(43)	P	−11.1	K(16)...F(20)+L(34)...G(38)	P	−11.8
	K(16)...E(22)	I	−10.0	V(40)...T(43)+Y(10)	I	−10.8	E(3)...R(5)	P	−11.7

<sup>a</sup>Letters **A**, **B** and **C** denote grid maps with different sizes (see Methods for letter codes). Location of the BSB peptides in the plane (I) or above/below the planes (P) of beta sheet of dimer is also marked (see text for further explanation of groups I and P of location).

amyloid. Significant energy differences were found for each active sequences, both for AAAAA (sequence A: 24–33 and 36–47%; sequence B: 24–29 and 22% differences with Tjernberg's and Soto's peptides, respectively; sequence C: 40% with Soto's peptide) and AAVFA (sequence A: 14 and 29%; with Tjernberg's and Soto's peptides, respectively; sequence B: 25% with Tjernberg's peptide; sequence C: 26% with Soto's peptide; in percentage of the BSB's energy which were lower than the blanks' in all cases). These considerable energy contributions refer to the importance of the role of the side chains in the interactions of the complexes. This finding is in good agreement with the experimental data published in ref 7 and supports the significance of our docked results.

**Preliminary molecular dynamics simulations.** During MD calculations all BSB peptides were moving together with the beta amyloid peptides. Dissociation was not observed. The electrostatic and hydrophobic interactions were stable in the time average. Although the terminus and the turn region of the amyloid peptide were moving intensively, the binding of the small BSB peptides was stable during the simulation time. Detailed analysis and binding free energy calculations of the studied complexes will be published elsewhere. (It should be remarked, that the complexes of Scheme 1A have survived the conditions of a force-field (GROMACS) which has different parameter set compared to the AMBER-based AutoDock parameters.)

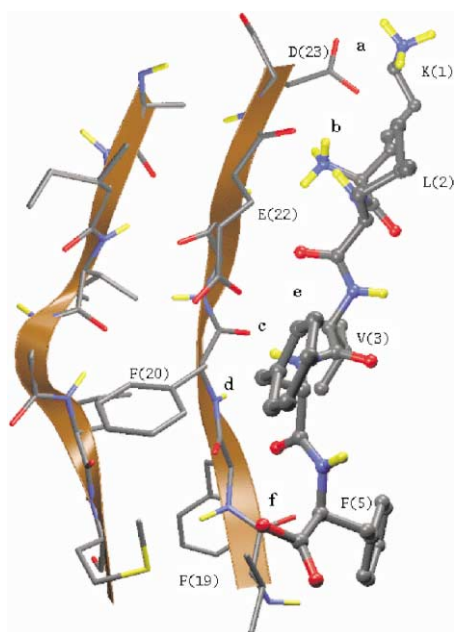


**Figure 1.** 3D structure of the complex formed by KLVFF peptide and the active sequence V(18)...D(23) (sequence 'A' on Scheme 1A) of the monomer A $\beta_{1-43}$  (target). KLVFF and the active fragment are in 'antiparallel' orientation, which finding is in good agreement with the statements of ref 12. Salt bridges **a** and **b** have distances of 3.11 and 2.95 Å between O and N atoms. H-bond **c** has an N...O distance of 3.01 Å and O...N...H angle: 42.7°. Aromatic (**d**) and hydrophobic interactions between V(18) and F(5) and two dipole–dipole interactions (**e** and **f**) are strengthening the complex.

### Docking of Tjernberg's peptide (KLVFF) and Soto's peptide (LPFFD) to the dimer of A $\beta_{1-43}$ (Target II)

Docking of BSB peptides on amyloid monomer serve as a possible model of interaction of BSBs and A $\beta_{1-43}$ , before aggregation and after breaking the oligomeric forms of amyloid. However, it is also important to know how BSB peptides could act on aggregated forms of the A $\beta_{1-43}$ . A simple dimer model was chosen in our investigations, which is indeed a piece of the 'solid-state model' published by George and Howlett.<sup>9</sup> The results of the docking experiments on this target are listed in Table 2. The active sequences of A $\beta_{1-43}$  could be divided roughly into two groups according to the location of BSB peptides: (1) in the plane of and (2) above or below the plane of the dimer amyloid associate. Representative sequences of group 1: (A) D(7)...Y(10)+T(43); (B) K(16)...E(22). Some important sequences of group 2: (A) D(1)...R(5); (B) Y(10)...H(13)+V(40)...T(43); (C) K(16)...V(18)+V(36)...G(37). There is one more sequence which belong to both groups, according to the BSBs' position: (D) S(8)...E(11)+V(40)...T(43) (Scheme 1B).

**Group 1.** (A) The D(7)...Y(10)+T(43) sequence of group 1 is a possible Achilles' heel of the dimer of A $\beta_{1-43}$ . It is located at the middle part of the dimer and contains several amino acids which could be easily involved in the interaction with a BSB peptide. Complex of this sequence with Soto's LPFFD is represented in Figure 3. (B) The interaction of BSBs with the K(16)...E(22) fragment of amyloid seems to be important in the stabilization of the amyloid–BSB

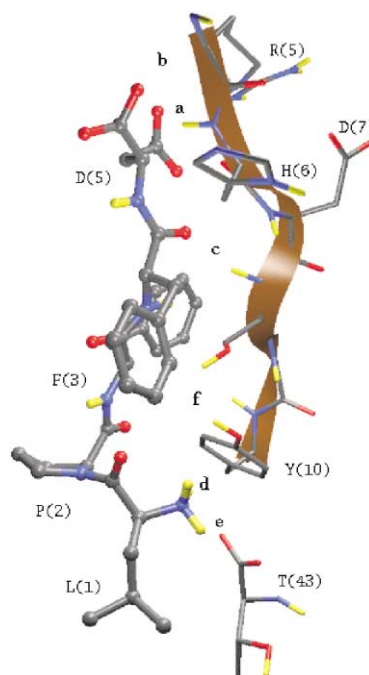


**Figure 2.** 3D structure of the LPFFD–A $\beta_{1-43}$  complex. A salt bridge (**e**) and hydrogen bonds (**a**, **b**, **c**, **d**, **f**) are involved in the interaction of LPFFD and R(5)...Y(10)+T(43) (sequence 'B' on Scheme 1A).

complex, that is after ‘beta-sheet breaking’ these interactions may help to keep the amyloid in non-aggregated form. This hypothesis is suggested by the arrangement of the BSB on this sequence: it is located beside the amyloid chain (Fig. 4). It should be mentioned, that KLVFF had a similar position on the monomer amyloid, as well [see Fig. 1 and the previous section for the details of importance of K(16)...E(22) sequence].

**Group 2.** (A) The N-terminal *D*(1)...*R*(5) fragment of  $\beta A_{1-43}$  contains three charged residues (Asp, Glu, Arg) and the charged amino group which make this sequence an attractive region for the charged amino acids of BSB peptides. However, no other types of interactions in the docked complex of this sequence and the BSBs could be observed. (B) The main interactions between Y(10)...H(13)+V(40)...T(43) parts of amyloid and Soto’s LPFFD are: three hydrogen bridges [Y(10)...L(1) of 2.69 Å and 37.7°; E(11)...F(4) of 3.16 Å and 42.5°; D(5)...H(13) of 3.48 Å and 23.43°] and the interaction between F(4) and the hydrophobic pocket formed by H(13) and V(40). (C) Formally, K(16)...V(18) sequence belongs to this group too. Together with V(40)...T(43)] sequence it forms a complex with BSBs in which the BSBs are sitting on the plane of the amyloid dimer. However, in these complexes there are no aromatic (and other specific) interactions with the amyloid, so these are basically different from the others of Group 1/B. (D) KLVFF and LPFFD are located around the C-terminal part (in and out of plane of  $\beta A_{1-43}$ ) of the amyloid at S(8)...E(11)+V(40)...T(43) sequences. Similar interactions occur in these complexes as in the case of (B) in group 2.

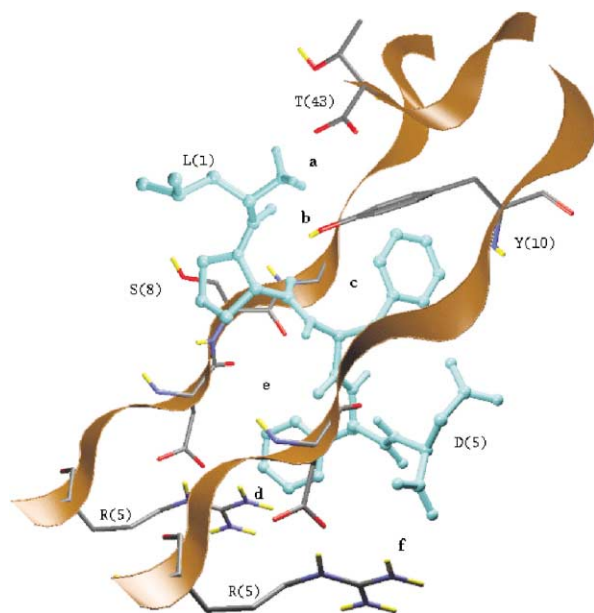


**Figure 3.** 3D structure of complex of LPFFD and the active part (1/A in Scheme 1B) of the dimer form of  $A\beta_{1-43}$  (target). Salt bridges (a: 2.47 Å; f: 4.62 Å); H-bridges (e.g., b: 2.49 Å and 49.0°; c, d: aromatic H-bridges of ca. 3 Å) and a dipole–dipole interaction (e) are stabilizing the BSB-amyloid complex.

## Conclusions

The development and testing of BSB peptides is a promising possibility of the research of anti-aggregating drugs against Alzheimer’s disease.<sup>16</sup> A lot of experiments were performed in vitro and in vivo to investigate and prove the effect of the two potent peptides: LPFFD<sup>8</sup> and KLVFF.<sup>7</sup> However, the mechanism of action of these peptides, that is the interactions with their target, the  $A\beta_{1-42/3}$  peptide has not been thoroughly studied.

In the present study, a relatively fast method: molecular docking was used for the mapping of the possible interactions of BSBs and their amyloid target. Here, we applied the algorithm in a fully automated way, that is, no experimental prediction for the binding sites on  $A\beta_{1-43}$ ; no information about the possible sites was available for the inputs of the calculations (see Methods for details). During the docking simulations a computationally derived model was used as a target molecule. This molecule involves the main secondary structural features of the amyloid peptide according to the recent literature, and therefore, could serve as a reliable target. [However, a detailed molecular dynamical investigation of the amyloid and its complexes (with itself and the BSBs) was done to get a full picture of the possible changes of the secondary structure in solution. Preliminary evaluation of these calculations verified the stability of the docked complexes presented in this study.]

Our results are in good agreement with experimental data: the V(18)FFAED(23) sequence was found by Tjernberg’s KLVFF peptide with quite good energy scores and frequencies. The high affinity of this sequence [with V(18)FF(20) central amino acids] to itself was shown recently<sup>12</sup> (see Results and Discussion for details).

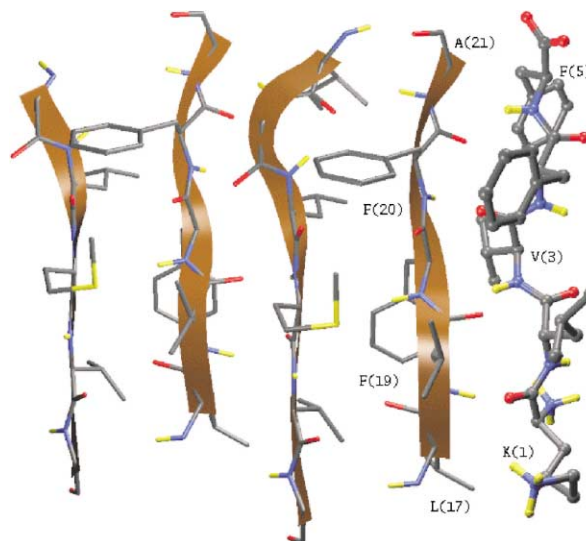


**Figure 4.** Orientation of KLVFF peptide on the active fragment of  $A\beta_{1-43}$  (target; 1/B on Scheme 1B) molecule. KLVFF is positioned beside the active K(16)...E(22) sequence, in the plane of amyloid, similarly to Figure 1.



Some other possible binding sequences were also identified, for example the final G(38)...T(43) part of the amyloid molecule which is also known to be essential in the aggregation mechanism of A $\beta$ <sub>1–42</sub><sup>13–15</sup> and according to the present studies it plays an important role in the interaction with the two BSB peptides.

D(7)...Y(10)+T(43) sequences were found to be active for both the monomer and dimer amyloid target [starting from E(3)...R(5) in the case of the monomer]. The aforementioned final sequences G(38)...T(43) have also occurred in the case of the dimer. These matching fragments may be essential in the ‘beta-sheet breaking’ effect of KLVFF and LPFFD: deaggregating the oligomers to monomers and/or inhibiting the formation of polymers.

## Methods

### Preparation of ligand and target molecules

Molecular structures of KLVFF (Tjernberg’s), LPFFD (Soto’s) peptide (ligand molecules) and AAAAA, AAVFA (blank ligands) were generated with the aid of PROTEIN program and optimised by NEWTON program of TINKER<sup>17</sup> program package with 0.001 kcal mol<sup>–1</sup> tolerance, using AMBER<sup>18</sup> force field parameters. The structure of A $\beta$ <sub>1–43</sub> peptide and the crystallographic parameters of the ‘solid-state model’<sup>9</sup> of amyloid plaques were kindly provided by Dr. D. R. Howlett (SmithKline Beecham Pharmaceuticals, Harlow, Essex, UK). The A $\beta$ <sub>1–43</sub> peptide (a monomer unit) was used as target during the simulations (Target I). ‘Solid-state’ form of A $\beta$ <sub>1–43</sub> peptide aggregate was built with the aid of program O<sup>19</sup> and a piece of this ‘crystal’ (containing two A $\beta$ <sub>1–43</sub> molecules) was used as ‘dimeric’ target (Target II). A $\beta$ <sub>1–43</sub> molecules were equipped with polar (essential) hydrogen atoms and charges of the Kollman united-atom type. Empirical partial charges of Gasteiger and Marsilli<sup>20</sup> were added to ligand pdb files. The charges of non-polar hydrogen atoms were united with the charges of the connecting carbon atoms with the aid of AutoTors<sup>21</sup> (the corresponding pdb coordinates of the H-atoms were eliminated in the same way). Atomic solvation parameters and fragmental volumes were assigned using Addsol.<sup>21</sup>

### Docking procedure

The AutoDock 3.0 program package<sup>21</sup> was used for the computational simulations. Mass-centered grid maps were generated by AutoGrid program with different sizes (volumes) and grid spacings (A: 120×30×30 for Target I, 120×120×120 for Target II and 0.75 Å; B: 200×90×90 for Target I, II and 0.55 Å; C: 170×55×55 for Target I, 170×60×70 for Target II and 0.55 Å). Weighed AMBER force field-based 12-10 and 12-6 Lennard–Jones parameters (supplied with the program package) were used for modelling H-bonds and van der Waals interactions, respectively. Distance dependent relative permittivity of Mehler and Solmajer<sup>22</sup> was applied in the calculation of electrostatic grid maps. One hundred separate docking runs were performed using the Lamarckian Genetic Algorithm (LGA) of the

program package. The maximum number of energy evaluations was set to 1.5 million per run, the initial translation, quaternion parameters and torsions of the ligands were randomized before each run (i.e., the ligand maneuvered to the binding site of the target starting from a random initial position and orientation). The rotation of  $\Phi$  and  $\Psi$  angles and the angles of the side chains were held free during the calculations. All other LGA parameters were set as default.

### Evaluation of results of docking simulations. Target I.

The resultant 100 docked conformation of the ligand peptides were listed in increasing energy order. The structures with the lowest 25 docked energies were used as a reference for grouping the 100 structures in the following way: (1) the distance between the mass centums of the reference structures and the others’ were calculated; (2) the structures were put in the same group if the distance between their mass centums was in 3 Å. The lowest energy conformation of each group was used for further characterization of the binding position (i.e., determination of the interacting sequences of the A $\beta$ <sub>1–43</sub> monomer). The interacting sequences, the number (*N*) of the conformations in each group and the docked energies of the BSB (ligand) peptide–A $\beta$ <sub>1–43</sub> peptide complexes are listed in Table 1. (Groups having total population less than two, are not presented in the table.)

*Target II.* Sequences corresponding to the BSB–A $\beta$ <sub>1–43</sub> complexes with the lowest 10 energies out of 100 were used for evaluation and listed in Table 2. (Identical sequences were listed only once.)

*Molecular dynamics.* Possible changes in the structures of the complexes (obtained by docking) were studied by 1 ns long molecular dynamics calculations using GROMACS (modified GROMOS87) force-field implemented in the GROMACS package.<sup>23</sup> 3-3 associates of the beta amyloid and the Tjernberg’s and Soto’s peptides (at sequences A, B and C) with the best energy scores of Autodock were used as initial structures. The preparation of the productive molecular dynamics runs was the same as before.<sup>24</sup> The complexes of Tjernberg’s and Soto’s peptides were solvated in 10245 SPC/E water molecules with 2 Na<sup>+</sup> counter ions and 10238 SPC/E water molecules with 4 Na<sup>+</sup> counter ions. In the 1 ns long productive MD calculations Particle Mesh Ewald (PME) method was used for the calculation of the long range electrostatic interactions in the periodic box. The possible shifts of the small BSB peptides on the beta amyloid peptides were measured by the distances between the functional groups.

The VMD<sup>25</sup> program was used for graphical interpretation and representation of results. Image rendering was made by Raster 3D.<sup>26</sup>

## Acknowledgements

This work was supported by the OTKA F035254 Hungarian Research Grant. The authors would like to thank Dr. D. R. Howlett for the crystallographic data of the

‘solid state model’ of amyloid. David Gatchell is acknowledged for linguistical corrections of the manuscript.

### References and Notes

- Jarrett, J. T.; Lansbury, P. T., Jr. *Biochemistry* **1992**, *31*, 12345.
- Selkoe, D. *Nature* **1999**, *399* (Suppl. 6738), A23.
- Benzinger, T.; Gregory, D.; Burkoth, T.; Miller-Auer, H.; Lynn, D.; Botto, R.; Meredith, S. *Proc. Natl. Acad. Sci. U.S.A.* **1998**, *95*, 13407.
- Tjernberg, L.; Callaway, D.; Tjernberg, A.; Hahne, S.; Liliehook, L.; Terenius, J.; Thyberg, C.; Norstedt, C. *J. Biol. Chem.* **1999**, *274*, 12619.
- Serpell, L. C. *Biochim. Biophys. Acta* **2000**, *1502*, 16.
- Findeis, M. A. *Biochim. Biophys. Acta* **2000**, *1502*, 76.
- Tjernberg, L.; Näslund, J.; Lindqvist, F.; Johansson, J.; Karlström, A. R.; Thyberg, J.; Terenius, L.; Nordstedt, C. *J. Biol. Chem.* **1996**, *271*, 8545.
- Soto, C.; Sigurdsson, E. M.; Morelli, L.; Kumar, R. A.; Castaño, E. M.; Frangione, B. *Nature Med.* **1998**, *4*, 822.
- George, A. R.; Howlett, D. R. *Biopolymers* **1999**, *50*, 733.
- Hilbich, C.; Kisters-Woike, B.; Reed, J.; Masters, C. L.; Beyreuther, K. *J. Mol. Biol.* **1992**, *228*, 460.
- Hetényi, C.; Körtvélyesi, T.; Penke, B. *J. Mol. Struct. (Theochem)* **2001**, *542*, 25.
- Balbach, J. J.; Ishii, Y.; Antzutkin, O. N.; Leapman, R. D.; Rizzo, N. W.; Dyda, F.; Reed, J.; Tycko, R. *Biochemistry* **2000**, *39*, 13748.
- Barrow, C. J.; Zagorski, M. G. *Science* **1991**, *253*, 179.
- Jarrett, J. T.; Lansbury, P. T., Jr. *Cell* **1993**, *73*, 1055.
- Snyder, S.; Lador, U.; Wade, W.; Wang, G.; Barrett, L.; Matayoshi, E.; Huffaker, H.; Kafft, G.; Holzman, T. *Biophys. J.* **1994**, *67*, 1216.
- Soto, C.; Saborio, G. P.; Permann, B. *Acta Neurol. Scand.* **2000**, *176* (Suppl.), 90.
- Dudek, M. J.; Ramnarayan, K.; Ponder, J. W. *J. Comp. Chem.* **1998**, *19*, 548.
- Cornell, W. C.; Cieplak, P.; Bayly, C. I.; Gould, I. R.; Merz, K. M., Jr.; Ferguson, D. M.; Spellmeyer, D. C.; Fox, T.; Caldwell, J. W.; Kollman, P. A. *J. Am. Chem. Soc.* **1995**, *117*, 5179.
- Jones, T. A. *Program O 7.0*; DatOno AB: Uppsala, Sweden.
- Gasteiger, J.; Marsili, M. *Tetrahedron* **1980**, *36*, 3219.
- Morris, G. M.; Goodsell, D. S.; Halliday, R. S.; Huey, R.; Hart, W. E.; Belew, R. K.; Olson, A. J. *J. Comp. Chem.* **1998**, *19*, 1639.
- Mehler, E. L.; Solmayer, T. *Protein Eng.* **1991**, *4*, 903.
- Lindahl, E.; Hess, B.; van der Spoel, D. *J. Mol. Model* **2001**, *7*, 306.
- Körtvélyesi, T.; Murphy, R. F.; Lovas, S. *J. Biomol. Struct. Dyn.* **1999**, *17*, 393.
- Humphrey, W.; Dalke, A.; Schulten, K. *J. Mol. Graph.* **1996**, *14*, 33.
- Merritt, E. A.; Bacon, D. J. *Methods Enzymol.* **1997**, *277*, 505.